Original Article
cnj.araku.ac.ir

☑ Cite This: Colloid Nanosci. J. 3(2) (2025) 595-601 DOI: 10.61882/CNJ.3.2.595

# Innovative Green Synthesis of Iron Oxide Nanoparticles Using Kelussia odoratissima Mozaff Extract and Their Antimicrobial Activity

***Atefeh Salehi[1], Sabah Salahvarzi[2]* , Mohammad Hadi Meshkatalsadat[1], Tayebeh Momeni[1]***

*[1]Department of chemistry, Qom university of technology, Qom, Iran.*
*[2]Department of Chemistry, Khor.C., Islamic Azad University, Khorramabad, Iran.*

**ARTICLE INFO**

***Article History:***
*Received 2025-08-30*
*Revised 2025-10-13*
*Accepted 2025-11-06*

***Corresponding Authors:***
*Sabah Salahvarzi*
*Email:*
*sabahsalahvarzi@iau.ac.ir*

**ABSTRACT**

Nanotechnology utilizes green synthesis methods for the production of iron oxide nanoparticles (Fe oxide NPs), favored for their low cost and high efficiency in large-scale industrial applications. In this study, iron oxide NPs were synthesized via a simple biological method using the aqueous extract of Kelussia odoratissima Mozaff leaves. The synthesized nanoparticles were characterized by UV-Vis spectroscopy, which showed an absorption peak at 220 nm, consistent with previous reports of green-synthesized iron oxide NPs. FTIR analysis revealed characteristic peaks at 3430 $cm^{-1}$ (O-H), 590 $cm^{-1}$ (Fe-O), 1600 $cm^{-1}$ (C=C), and 900 $cm^{-1}$ (C–H out-of-plane bending vibrations), indicating the presence of functional groups responsible for nanoparticle formation and stabilization. SEM imaging showed spherical nanoparticles with an average size ranging from 27 to 33 nm. XRD patterns confirmed the crystalline hexagonal rhombohedral phase of α-$Fe_2O_3$ with main diffraction peaks at 24.1°, 33.2°, 35.6°, 49.5°, 54.1°, and 62.4°. The antimicrobial activity of the iron oxide NPs was tested against Escherichia coli and Candida albicans, revealing limited inhibition compared to the stronger effects observed with the original plant extract. These findings suggest that bioactive compounds in the Kelussia odoratissima extract play a significant role in antimicrobial activity, and further purification of the nanoparticles may enhance their efficacy.

**KEYWORDS:** *Kelussia odoratissima Mozaff. Leaf, Green synthesis, Iron Oxide Nanoparticle, Escherichia coli, Candida albicans*

## 1. Introduction

Nanoparticles have been extensively researched due to their properties and size, and they are widely used in many applications. There are two types of nanoparticles: anthropogenic (like all manufactured nanoparticles) and natural (like soil colloids, biomagnetite)[1]. Based on the shape and structure, there are different types of nanoparticles such as clusters, biometallics, nanotubes and nanocubes [2]. Recently, different metal oxide nanoparticles like zinc, silver, magnesium, iron, gold, copper, cobalt, cesium and bismuth have been synthesized [3]. An essential metal oxide is Fe ONPs. Because of their vital role in the different process, cost-effectiveness and unique physicochemical properties (easy separation, biocompatibility, magnetic properties and stability), they have received special attention in science and technology [4]. iron oxide NPs have different applications in drug delivery, diagnosis, biomedicine and bioremediation [5-7]. There are different synthesis methods for the synthesis of iron oxide NPs nanoparticles, the best of that is the eco-friendly method [8]. Different synthesis methods like biological, electrochemical, photochemical and chemical methods have been investigated. Chemical synthesis routes are not cost-effective and consume

a lot of energy, the chemicals used are dangerous that cause adverse effects on living organisms, they cause a lot of damage to the environment, they have problems in biocompatibility and physicochemical properties, Although in this method is the short synthesis time [9,10]. Because of the disadvantages of the chemical method, the biological synthesis of iron oxide NPs was carried out using plant extracts or agricultural waste, which is environmentally friendly and cost-effective [11]. The bioactive compounds of plant extracts stabilize nanoparticles, are reducing and capping agents during synthesis, inhibit aggregation, and are beneficial for health. [12, 13]. Recently, The green synthesis of iron oxide NPs from different plants like Avicennia Marina Flower [14], Lagenaria Siceraria [15], Daphne mezereum [16], Mimosa pudica root [17], pomegranate seeds [18]. In this paper green synthesis of iron oxide NPs from Kelussia odoratissima Mozaff. Kelussia odoratissima Mozaff is native to Iran and is self-growing, fragrant and belongs to the Apiaceae family [19]. It is a glabrous, wild, perennial aromatic herb and erect, It has a length of 120 to 200 cm. It is called "Karafse-Koohi" in the local term. Kelussia odoratissima Mozaff., an endemic aromatic herb of Iran belonging to the Apiaceae family, is distinguished by its unique phytochemical composition. The plant is notably rich in bioactive compounds including phthalides, flavonoids, phenolic acids, and essential oils, which exhibit potent antioxidant and reducing properties. These compounds facilitate the green synthesis of iron oxide NPs by acting as natural reducing and capping agents, promoting effective reduction of iron ions and preventing nanoparticle aggregation. Particularly, the elevated levels of ferulic acid and Z-ligustilide present in K. odoratissima differentiate it from other commonly studied plants for nanoparticle synthesis. Despite these promising attributes, limited research has explored the application of K. odoratissima extract in nanoparticle fabrication, underscoring the novelty and significance of the present study. Kelussia odoratissima also exhibits anti-tussive, sedative, antioxidant, anti-inflammatory, and notable antimicrobial activities against pathogens such as Escherichia coli and Candida albicans [20]. In this paper, the green synthesis of iron oxide NPs is performed by the extract of Kelussia odoratissima Mozaff, and the properties of the particles are determined with different devices, and also their antibacterial activity is investigated. While some biosynthesized iron oxide nanoparticles may exhibit amorphous characteristics, in this study, the synthesized nanoparticles were found to possess a primarily crystalline structure corresponding to the $\alpha$-$Fe_2O_3$ phase, as confirmed by X-ray diffraction analysis. This crystalline nature is expected to influence their physicochemical and biological properties

## 2. Experimental

### *2.1. Materials and Methods*

Iron (III) chloride trihydrate [Fe(Cl3). 3H2O] and sodium hydroxide were procured from Merck (Germany). Solvents were purchased from Merck chemical company and used without any further purification. A Shimadzu spectrometer (UV-160A) was employed to perform UV-Vis at 200-1000 nm, a Thermo Avatar spectrometer to perform FT-IR, a SEM FEI Quanta 200 TESCAN Mira-3 to analyze the surface morphology and particle size. X-ray diffraction (XRD) analysis was carried out using a Philips PW 1730 diffractometer over a 2$\theta$ range of 20° to 80° at room temperature. The obtained XRD pattern exhibited sharp and well-defined peaks corresponding to the crystalline $\alpha$-$Fe_2O_3$ phase, confirming the predominantly crystalline nature of the synthesized nanoparticles

### *2.2. Synthesis and procedures*

#### *a. Preparation of Kelussia odoratissima Mozaff extract*

*Kelussia odoratissima* Mozaff was collected from Zagros mountains, some of its fresh leaves were washed with deionized water. Then, the leaves were dried at room temperature, and away from sunlight for a period of 5 days. Then 10 gr of the dried leaves of the plant are mixed with 90 ml of deionized water in an Erlenmeyer flask, then the resulting mixture was placed on a heater for 20 minutes and the resulting extract was filtered through filter paper after cooling until the solid particles are completely separated from it.

#### *b. Synthesis of iron oxide NPs*

A 0.01 M aqueous solution of iron(III) chloride hexahydrate ($FeCl_3{\cdot}6H_2O$) was prepared by dissolving the appropriate amount of salt in deionized water. The Kelussia odoratissima leaf extract was gradually added to the $FeCl_3$ solution in a 1:1 volume ratio under continuous stirring. The

pH of the reaction mixture was carefully adjusted to 9 by adding 0.1 M sodium hydroxide solution. The reaction was maintained at room temperature (25 ± 2 °C) with constant stirring for 2 hours. The gradual color change from yellow to reddish-brown signified the formation of iron oxide nanoparticles. Upon completion, the mixture was centrifuged at 12,000 rpm for 20 minutes, repeated three times. The collected precipitate was washed thoroughly—twice with 70% ethanol and three times with distilled water—to eliminate impurities, then dried at 60 °C for 12 hours before further analysis.

### *2.3. Antimicrobial Activity test*

The antimicrobial activity of synthesized iron oxide NPs using extract of Kelussia odoratissima Mozaff was investigated against two Candida albicans and Escherichia coli by using the method of disk diffusion; Empty antibiogram discs were immersed in the culture medium with different concentrations of the test sample (1000, 500, 250 µg/ml) for 5 minutes. Then, freshly cultured bacteria were mass cultured with sterile swap in Mueller Hinton agar culture medium. Then, the discs impregnated with different concentrations of the tested sample were placed in the agar medium at appropriate intervals and incubated for 24 hours in a 37degree incubator. Then, the diameter of the lack of growth halo was measured.

## 3. Results and Discussion

The UV-Vis absorption spectrum of the aqueous extract of *Kelussia odoratissima Mozaff* leaves exhibits a prominent absorption peak at 220 nm within the 200–500 nm wavelength range (Fig. 1). This peak is consistent with previously reported UV-Vis absorption characteristics of iron oxide nanoparticles synthesized via green methods, which commonly show absorption between 190 and 230 nm due to electronic transitions in $Fe^{3+}$ ions [15, 21]. Such absorption confirms the successful formation of iron oxide NPs and reflects the nanoscale size and surface plasmon resonance effects typical for these particles.

To further identify the biomolecules involved and confirm nanoparticle formation, Fourier-transform infrared (FT-IR) spectroscopy was employed (Fig. 2). The characteristic peak observed

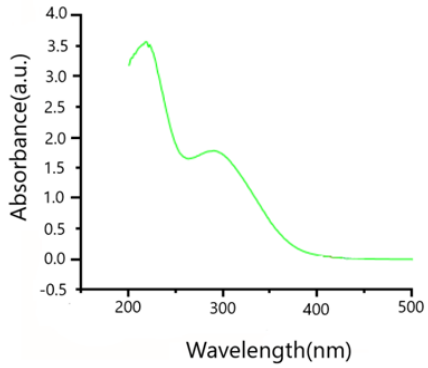


**Fig. 1.** UV–Vis spectra of iron oxide nanoparticlesNPs.

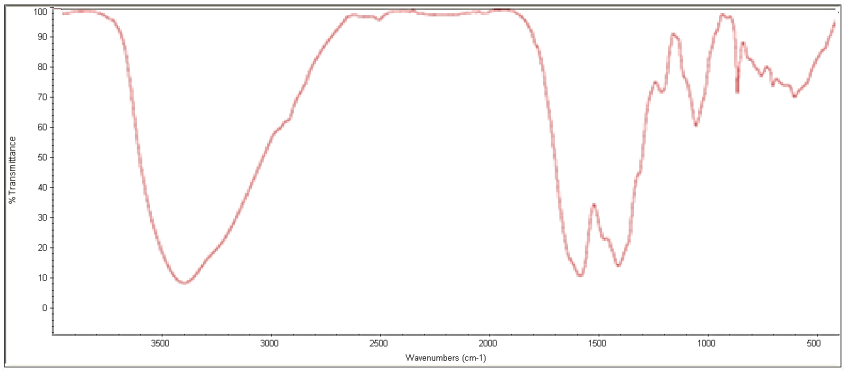


**Fig. 2.** FT-IR spectra iron oxide NPs synthesized from Kelussia odoratissima Mozaff extract.

at 590 $cm^{-1}$ corresponds to the stretching vibration of the Fe–O bond in the hematite ($\alpha$-$Fe_2O_3$) phase, consistent with literature reports [33]. A broad absorption band at 3430 $cm^{-1}$ is attributed to the O–H stretching vibrations of hydrogen-bonded hydroxyl groups, which likely arise from iron hydroxide species formed during the nanoparticle synthesis process as well as residual water molecules. The peak near 1600 $cm^{-1}$ corresponds to C=C stretching vibrations, indicating the presence of aromatic rings from phytochemical compounds.

Importantly, the sharp peak around 900 $cm^{-1}$ is assigned to C–H out-of-plane bending vibrations characteristic of aromatic compounds. This assignment aligns with the known phytochemical profile of Kelussia odoratissima, which is rich in flavonoids, phthalides, and other aromatic bioactive molecules. These compounds act as natural reducing and capping agents, facilitating the reduction of $Fe^{3+}$ ions and stabilizing the iron oxide NPs, preventing aggregation during synthesis. This observation supports the green synthesis route and highlights the dual role of the plant extract both in nanoparticle formation and stabilization. The FT-IR spectra thus confirm the successful biosynthesis of iron oxide NPs and their stabilization by bioactive natural compounds present in the *Kelussia odoratissima*.

SEM was performed to evaluate the morphology and particle size of iron oxide NPs. The electron microscope image showed the shape of iron oxide NPs to be spherical and its average size was 27-33 nanometers.

X-ray diffraction is used to determine the phase identity and crystal structure of nanoparticles. The crystal structure of the synthesized nanoparticles was shown by sharp and intense peaks in the XRD analysis (Figure 4) and they correspond to the standard values of α-Fe2O3 hexagonal rhombic phase (JCPDS-33-0664). The main diffraction peaks were observed at 2θ values of 24.1°, 33.2°, 35.6°, 49.5°, 54.1°, and 62.4° confirming the hexagonal rhombic phase.

The composition of iron oxide NPs synthesized using *Kelussia odoratissima* Mozaff extract was determined using EDS analysis. As can be seen in the spectra, the presence of iron oxide NPs was confirmed and the rest of the elements present are other elements of the plant. EDS spectra confirmed the presence of Fe and O, along with minor peaks

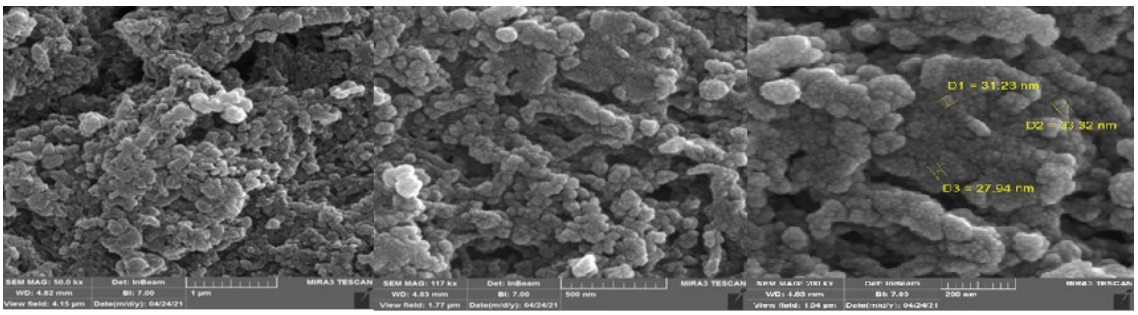


**Fig. 3.** SEM image of iron oxide NPs synthesized from Kelussia odoratissima Mozaff extract.

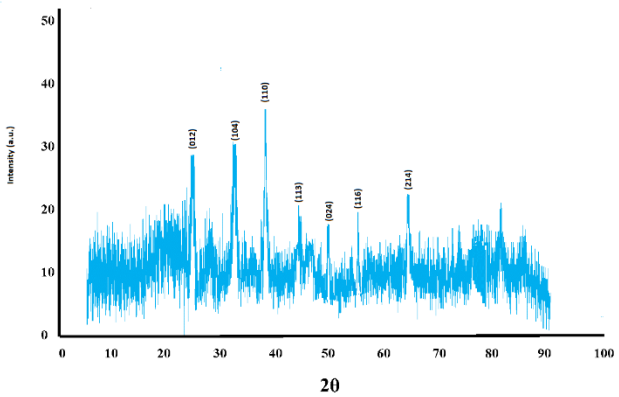


**Fig. 4.** XRD pattern of the green-synthesized iron oxide NPs.

from plant-derived elements such as C and N, consistent with previous green synthesis reports [22].

Although our iron oxide NPs exhibited only minimal antimicrobial activity under the tested conditions, previous studies have reported significant antibacterial effects of FeO and $Fe_3O_4$ nanoparticles against Escherichia coli and Candida albicans. The limited antimicrobial potential observed in our synthesized iron oxide NPs may be attributed to differences in synthesis parameters, surface characteristics, or the presence of residual plant compounds that interfere with nanoparticle–microbe interactions. Notably, the original Kelussia odoratissima extract demonstrated stronger antimicrobial

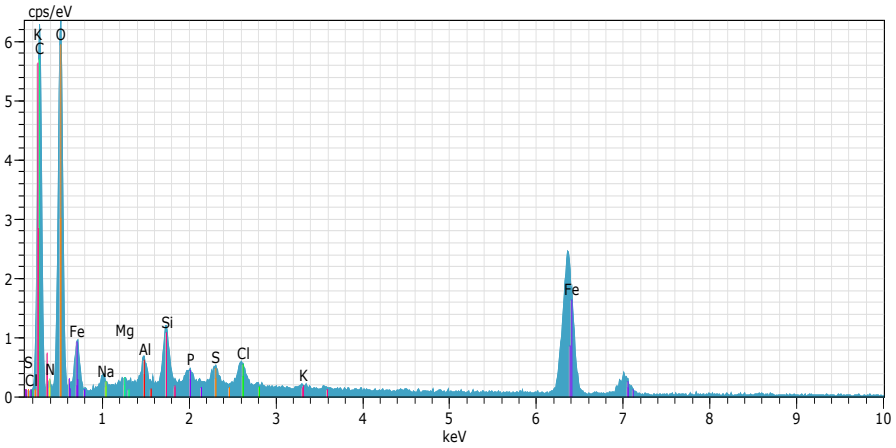


**Fig. 5.** EDS spectrum of iron oxide NPs.

**Table 1.** EDS data of iron oxide NPs synthesized from Kelussia odoratissima Mozaff extract.

| Element | Atomic Number | Series | Unnormalized Conc. (wt.%) | Normalized Conc. (wt.%) | Atomic Conc. (at.%) | Error (± wt.%) |
|---|---|---|---|---|---|---|
| O | 8 | K | 65.11 | 46.28 | 43.66 | 8.97 |
| C | 6 | K | 52.38 | 37.26 | 36.62 | 7.49 |
| Fe | 26 | K | 11.19 | 7.95 | 1.95 | 1.20 |
| N | 7 | K | 3.77 | 2.68 | 2.73 | 0.74 |
| Si | 14 | K | 3.14 | 2.23 | 1.09 | 0.63 |
| Na | 11 | K | 2.65 | 1.89 | 1.53 | 0.58 |
| Al | 13 | K | 1.63 | 1.16 | 0.56 | 0.41 |
| S | 16 | K | 0.90 | 0.64 | 0.25 | 0.28 |
| Mg | 12 | K | 0.22 | 0.16 | 0.14 | 0.09 |
| P | 15 | K | 0.19 | 0.14 | 0.09 | 0.08 |
| K | 19 | K | 0.10 | 0.07 | 0.05 | 0.06 |
| Total | | | 140.68 | 100.00 | 100.00 | |

**Table 2.** Antibacterial Activity of the Sample Against E. coli at Various Concentrations (Disk Diffusion Method)

| Sample Code | Concentration (µg/ml) | Inhibition Zone Diameter (mm) |
|---|---|---|
| SA9 | 1000 | 0 |
| SA9 | 500 | 0 |
| SA9 | 250 | 0 |

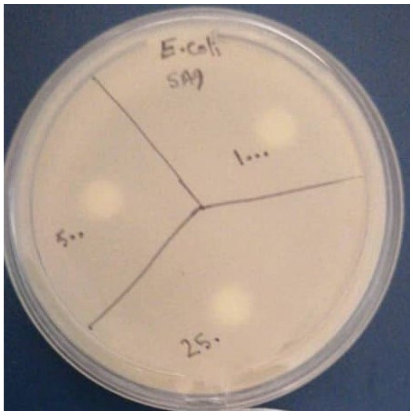


**Fig. 6.** Zone of inhibition test for bismuth sample against E. coli using standard antibiogram disks. All tested concentrations (1000, 500, 250 µg/ml) resulted in zero inhibition.

effects compared to the synthesized nanoparticles, suggesting that bioactive constituents in the extract play a more direct role in microbial inhibition. To enhance the efficacy of iron oxide NPs, future studies should aim to isolate and purify the active phytochemicals involved in nanoparticle synthesis, thereby minimizing the influence of plant-derived impurities on nanoparticle performance. The crystalline nature of the nanoparticles, confirmed by sharp XRD peaks corresponding to the α-$Fe_2O_3$ phase, along with their nanoscale size and spherical morphology observed by SEM, are important factors influencing their interaction with microbial cells. Crystallinity can affect surface reactivity, while smaller particle size increases surface area available for microbial interaction(Table2, Figure 6). However, in this study, despite these favorable properties, the antimicrobial activity remained limited, possibly due to surface charge effects or the presence of plant-derived compounds on the nanoparticle surface.

## 4. Conclusions

This study highlights the potential of Kelussia odoratissima Mozaff extract as a green, cost-effective, and non-toxic agent for the synthesis of iron oxide NPs. The resulting nanoparticles were spherical, crystalline, and approximately 31 nm in size. Despite the crystalline nature of the nanoparticles, no clear correlation between crystallinity and enhanced antimicrobial activity was observed, suggesting that further studies are needed to clarify the impact of nanoparticle structure on biological performance. Although the antimicrobial activity of the synthesized iron oxide NPs was evaluated, only minimal effects were observed under the tested conditions. These findings suggest that while the plant extract offers an eco-friendly route for nanoparticle production, further optimization is required to enhance the biological functionality of the resulting iron oxide NPs. Future studies should focus on refining synthesis parameters and isolating active phytochemicals to improve antimicrobial efficacy.

## Acknowledgement

The authors sincerely appreciate the support provided by Qom University of Technology and Islamic Azad University, Khorramabad, for facilitating this research.

## Disclosure Statement

No potential conflict of interest was reported by the authors.

## References

[1] Prajitha, N., Athira, S., Mohanan, P., Bio-interactions and risks of engineered nanoparticles, *Environ. Res.*, 172 (2019) 98–108. https://doi.org/10.1016/j.envres.2019.02.003

[2] De Marchi, L., Coppola, F., Soares, A.M., Pretti, C., Monserrat, J.M., Della Torre, C., Freitas, R., Engineered nanomaterials: From their properties and applications, to their toxicity towards marine bivalves in a changing environment, *Environ. Res.*, 178 (2019) 108683. https://doi.org/10.1016/j.envres.2019.108683

[3] Miri, A., Darroudi, M., Entezari, R., Sarani, M., Biosynthesis of gold nanoparticles using *Prosopis farcta* extract and it's in vitro toxicity on colon cancer cells, *Res. Chem. Intermed.*, 44 (2018) 3169–3177. https://doi.org/10.1007/s11164-018-3299-y

[4] Mishra, B., Varjani, S., Agrawal, D.C., Mandal, S.K., Ngo, H.H., Taherzadeh, M.J., Chang, J.-S., You, S., Guo, W., Engineering biocatalytic material for the remediation of pollutants: a comprehensive review, *Environ. Technol. Innov.*, 20 (2020) 101063. https://doi.org/10.1016/j.eti.2020.101063

[5] Varjani, S., Rakholiya, P., Shindhal, T., Shah, A.V., Ngo, H.H., Trends in dye industry effluent treatment and recovery of value added products, *J. Water Process Eng.*, 39 (2021) 101734. https://doi.org/10.1016/j.jwpe.2020.101734

[6] Selvinsimpson, S., Rani, S.E.G.D., Kumar, A.G., Rajaram, R., Lydia, I.S., Chen, Y., Photocatalytic activity of $SnO_2$/$Fe_3O_4$ nanocomposites and the toxicity assessment of *Vigna radiata*, *Artemia salina* and *Danio rerio* in the photodegraded solution, *Environ. Res.*, 195 (2021) 110787. https://doi.org/10.1016/j.envres.2021.110787

[7] Amit, C., Helly, C., Kumar, M.A., Varjani, S., Nanotechnological interventions for the decontamination of water and wastewater, *Water Wastewater Treat. Technol.*, (2019) 487–499. https://doi.org/ 10.1007/978-981-13-3259-3_22

[8] Pandian, A.M.K., Rajasimman, M., Rajamohan, N., Varjani, S., Karthikeyan, C., Anaerobic mixed consortium (AMC) mediated enhanced biosynthesis of silver nanoparticles (AgNPs) and its application for the removal of phenol, *J. Hazard. Mater.*, 416 (2021) 125717. https://doi.org/10.1016/j.jhazmat.2021.125717

[9] El-Shishtawy, R.M., Asiri, A.M., Al-Otaibi, M.M., Synthesis and spectroscopic studies of stable aqueous dispersion of silver nanoparticles, *Spectrochim. Acta A Mol. Biomol. Spectrosc.*, 79 (2011) 1505–1510. https://doi.org/ 10.1016/j.saa.2011.05.007

[10] Karuppannan, S.K., Dowlath, M.J.H., SB, M.K., GI, D.R., Subramanian, S., Arunachalam, K.D., Phytochemical and Antibacterial Activity of *Cardiospermum halicacabum* Against Wound Pathogens, *Pharmacogn. J.*, 12 (2020). https://doi.org/ 10.5530/pj.2020.12.179

[11] Elkhateeb, O., Atta, M.B., Mahmoud, E., Biosynthesis of iron oxide nanoparticles using plant extracts and evaluation of their antibacterial activity, *AMB Express*, 14 (2024) Article 92. https://doi.org/10.1186/s13568-024-01746-9

[12] Conde-Cid, M., Paíga, P., Moreira, M., Albergaria, J., Álvarez-Rodríguez, E., Arias-Estévez, M., Delerue-Matos, C., Sulfadiazine removal using green zero-valent iron nanoparticles: A low-cost and eco-friendly alternative technology for water remediation, *Environ. Res.*, 198 (2021) 110451 https://doi.org/10.1016/j.envres.2020.110451

[13] Kharissova, O.V., Dias, H.R., Kharisov, B.I., Pérez, B.O., Pérez, V.M.J., The greener synthesis of nanoparticles, *Trends Biotechnol.*, 31 (2013) 240–248. https://doi.org/10.1016/j.tibtech.2013.01.003

[14] Karpagavinayagam, P., Vedhi, C., Green synthesis of iron oxide nanoparticles using *Avicennia marina* flower extract, *Vacuum*, 160 (2019) 286–292. https://doi.org/10.1016/j.vacuum.2018.11.043

[15] Kanagasubbulakshmi, S., Kadirvelu, K., Green synthesis of iron oxide nanoparticles using *Lagenaria siceraria* and evaluation of its antimicrobial activity, *Def. Life Sci. J.*, 2 (2017) 422–427. https://doi.org/ 10.14429/dlsj.2.12277

[16] Beheshtkhoo, N., Kouhbanani, M.A.J., Savardashtaki, A., Amani, A.M., Taghizadeh, S., Green synthesis of iron oxide nanoparticles by aqueous leaf extract of *Daphne mezereum* as a novel dye removing material, *Appl. Phys. A*, 124 (2018) 1–7. https://doi.org/ 10.1007/s00339-018-1782-3.

[17] Niraimathee, V., Subha, V., Ravindran, R.E., Renganathan, S., Green synthesis of iron oxide nanoparticles from *Mimosa pudica* root extract, *Int. J. Environ. Sustain. Dev.*, 15 (2016) 227–240. https://doi.org/10.1504/IJESD.2016.077370

[18] El-Kassas, H.Y., Aly-Eldeen, M.A., Gharib, S.M., Green synthesis of iron oxide ($Fe_3O_4$) nanoparticles using two selected brown seaweeds: Characterization and application for lead bioremediation, *Acta Oceanol. Sin.*, 35 (2016) 89–98. https://doi.org/0.1007/s13131-016-0880-3

[19] Azizi, M., Mashreghi, M., Oroojalian, F., Shahyahmasebi, N., Antibacterial activities of *Kelussia odoratissima* and *Teucrium polium* essential oils in combination of synthetic silver nanoparticles against food-borne pathogens, *J. Hortic. Sci.*, 30 (2016). https://doi.org/10.22067/jhorts4.v30i2.40634

[20] Yazdani, Z., Shakerian, A., Rahimi, E., Jafarian Dehkordi, M., Sharafati Chaleshtori, R., Antibacterial activities of *Kelussia odoratissima* and *Echinophora platyloba* extracts and essential oils against waterborne pathogens, J. Med. Plants Biotechnol., 2 (2024) 43–52. https://doi.org/10.22034/jmpb.2024.365156.1664

[21] Gök, M., Yıldız, A., Amino acid-assisted synthesis and characterization of iron-containing nanoparticles for bio-interaction studies with *Metschnikowia* spp., *Glob. Sci. Technol. Appl. Eng. Technol.*, 2 (2022) 43–52. https://doi.org/10.30574/gscaet.2022.4.1.0043

[22] Liu, X., Zhang, J., Wu, S., Yang, D., Liu, P., Zhang, H., Wang, S., Yao, X., Zhu, G., Zhao, H., Single crystal α-$Fe_2O_3$ with exposed {104} facets for high performance gas sensor applications, *RSC Advances*, 2 (2012) 6178–6184. https://doi.org/10.1039/C2RA20797D